

1 **Trawling-induced daily sediment resuspension in the flank of a Mediterranean**  
2 **submarine canyon**

3

4 Jacobo Martín\*, Pere Puig, Albert Palanques, Marta Ribó

5

6 Institut de Ciències del Mar (CSIC), Passeig Marítim de la Barceloneta, 37-49, 08003

7 Barcelona, Spain.

8

9 \*Corresponding author: [jmartin@icm.csic.es](mailto:jmartin@icm.csic.es);

10 Tf: +33 932309500(ext.1156); fax: +33 932309555

11

12 **Abstract**

13

14 Commercial bottom trawling is one of the anthropogenic activities causing the biggest impact  
15 on the seafloor due to its recurrence and global distribution. In particular, trawling has been  
16 proposed as a major driver of sediment dynamics at depths below the reach of storm waves,  
17 but the issue is at present poorly documented with direct observations. This work analyses  
18 changes in water turbidity in a tributary valley of the La Fonera (=Palamós) submarine  
19 canyon, whose flanks are routinely exploited by a local trawling fleet down to depths of 800  
20 m. A string of turbidimeters was deployed at 980 m water depth inside the tributary for two  
21 consecutive years, 2010-2011. The second year, an ADCP profiled the currents 80 m above  
22 the seafloor. The results illustrate that near-bottom water turbidity at the study site is heavily  
23 dominated, both in its recurrence and its magnitude and temporal patterns, by trawling-  
24 induced sediment resuspension at the fishing ground. Resuspended sediments are channelized  
25 along the tributary in the form of sediment gravity flows, being recorded only during working

26 days and working hours of the trawling fleet. These sediment gravity flows generate turbid  
27 plumes that extend to at least 100 m above the bottom, reaching suspended sediment  
28 concentrations up to 236 mg l<sup>-1</sup> close to the seafloor (5 m above bottom). Few hours after the  
29 end of daily trawling activities, water turbidity progressively decreases but resuspended  
30 particles remain in suspension for several hours, developing bottom and intermediate  
31 nepheloid layers that reach background levels ~2 mg l<sup>-1</sup> before trawling activities resume the  
32 day after. The presence of these nepheloid layers was recorded in a CTD+turbidimeter  
33 transect conducted across the fishing ground few hours after the end of a working day. These  
34 results highlight that deep bottom trawling can effectively replace natural processes as the  
35 main driving force of sediment resuspension on continental slope regions and generate  
36 increased near-bottom water turbidity that propagates from fishing grounds to wider and  
37 deeper areas via sediment gravity flows and nepheloid layer development.

38

39 Keywords: Trawling; Man-induced effects; Submarine canyons; Sediment dynamics;  
40 Resuspension; Nepheloid layers; Northwestern Mediterranean

41

42

43

44

45

46

47

48

49

50

51

52 **1. Introduction**

53

54 Bottom trawling is a fishing technique that consists in pulling nets along the seafloor to  
55 harvest benthic and demersal living resources. The means to keep the net open and close to  
56 the bottom are diverse but invariably imply the use of heavy devices such as otter boards,  
57 bobbins, sweepnet lines or chains, that are in contact with the seafloor continuously or  
58 intermittently. In certain cases, beams or dredges designed to actively bulldoze the seafloor  
59 are used. Aside from the direct impacts on benthic fauna and their habitats, the dragging of  
60 these gears along the seafloor injects large amounts of surface sediments into the water  
61 column, particularly when trawling is carried out over soft bottoms (Black and Parry, 1994;  
62 Pilskaln et al., 1998). In fact, in certain trawling modalities such as otter trawling, the clouds  
63 of resuspended sediments constitute an integral part of the fishing strategy by “herding” fish  
64 swarms towards the mouth of the net (Main and Sangster, 1981). Given the global dimension  
65 and recurrence of commercial trawling (World Resources Institute, 2000; Bensch et al., 2009;  
66 Puig et al., 2012), the question arises whether this human activity can make a sizeable  
67 contribution to present-day sediment resuspension and water column turbidity over extensive  
68 areas of the world’s continental margins. Churchill (1989) brought the issue into focus,  
69 proposing that trawling activities were able to rival storms as the main agent for sediment  
70 resuspension and transport on the middle and outer continental shelf of the Middle Atlantic  
71 Bight. More than 20 years after this pioneering work, the body of literature addressing this  
72 subject is still relatively slim and mainly devoted to coastal and continental shelf settings  
73 (Pilskaln et al., 1998; Palanques et al., 2001; Durrieu de Madron et al., 2005; Tragou et al.,  
74 2005; Dellapenna et al., 2006; Ferré et al., 2008), which leaves a big gap of knowledge on the  
75 effects of this practice at depths beyond the shelf-break. Filling this gap is a pressing issue

76 because of two overlapping factors. First, bottom fisheries have progressively extended their  
77 activities from traditional shallow grounds towards the continental slope and further offshore  
78 during the last decades (Morato et al. 2006, Bensch et al., 2009; Benn et al., 2010). Second, it  
79 is generally agreed (though scarcely documented) that artificial disturbances of the seafloor  
80 tend to be more severe and long-lasting in deep-sea than in shallow water environments, due  
81 to the fact that the natural processes capable of overcoming human imprints are in general  
82 weaker in the former (Theil and Schriever, 1990; Kaiser et al., 2002).

83

84 Among deep-sea environments susceptible of being impacted by trawl industries, submarine  
85 canyons are regarded as relevant and fragile hotspots of biodiversity (WWF/IUCN, 2004;  
86 Fabri et al., 2013). Canyons incising the continental shelf act as preferential routes and/or  
87 traps for organic and inorganic particulate matter from both terrestrial and marine sources.  
88 Also, by promoting local upwelling, canyons can be sites of enhanced biological production  
89 (Allen et al., 2001). Their complex morphology offers diverse habitats and shelter to marine  
90 species, including some of high economic value and, consequently, prosperous fishing  
91 harbours are often based in the vicinity of submarine canyons (Würtz, 2012). La Fonera  
92 Canyon, also known as Palamós Canyon (Fig. 1), is one of the most prominent submarine  
93 canyons of the northwestern Mediterranean (Palanques et al., 2005; Martín et al., 2006;  
94 Lastras et al., 2011). Its flanks from ~400 to 800 m depth are intensely exploited by a local  
95 trawling fleet targeting the blue and red shrimp *Aristeus antennatus*. Trawlers are active on a  
96 daily basis and year round, except for weekends and holidays, mainly along the Sant Sebastià  
97 fishing ground in the northern canyon flank (Fig. 1). The same ground is usually swept  
98 several times a day, starting typically at 6-7 h (UTC) in an offshore direction. Subsequent  
99 hauls may be carried out until 15-16 h, when the boats head back to port. The bottom trawl  
100 gear used in this fishery consists of 2 otter boards, each up to 1 ton in weight, spread ~100 m

101 apart during the trawling operation and connected to the net opening by 60-200 m-long  
102 sweeplines. The net measures 80-150 m in length and is ~50 m wide at its ballasted mouth.  
103 The daunting capacity of these otter trawling gears to resuspend big volumes of sediments is  
104 not new to fishermen: small trawlers' crews complain about their nets being clogged -and thus  
105 inoperative- by the mud propelled on the wake of the bigger trawlers sailing ahead (Alegret  
106 and Garrido, 2004). Studies conducted in 2001 showed that trawling gears operating in the  
107 Sant Sebastià fishing ground were able to trigger sediment gravity flows that were funnelled  
108 through a tributary valley (named Montgri) and were observed reaching the main canyon axis  
109 at 1200 m depth (Palanques et al., 2006; Martín et al., 2007). Further studies also documented  
110 the consequences of these man-made flows in terms of downward sediment fluxes and  
111 sediment accumulation rates in the canyon axis (Martín et al., 2006, 2008). Recently, Puig et  
112 al. (2012) evidenced that the periodic sediment removal from La Fonera Canyon fishing  
113 grounds ultimately reshaped the continental slope morphology over large spatial scales.

114

115 This paper aims to improve our understanding of trawling-induced sediment resuspension  
116 events along the northern canyon flank, describing in detail the daily and seasonal variability  
117 of water turbidity and discussing also the implications of such resuspension process in the  
118 generation of nepheloid layers along continental margins.

119

120

121

122

123

124

125

## 126 **2. Materials and methods**

127

128 An instrumented mooring array was deployed in the Montgrí tributary traversing the northern  
129 flank of the La Fonera Canyon (red diamond in Fig. 1). The mooring line was positioned at  
130  $41^{\circ}52.49'N$ ;  $3^{\circ}20.66'E$ , in a water depth of 980 m, ~200 m deeper than the maximum  
131 working depth of the local trawling fleet, during two consecutive years. From 1 July to 7  
132 November 2010, the line was equipped with 10 Seapoint turbidimeters (AQUA logger 520,  
133 AQUATEC; wavelength 880 nm, scatterance angles 15-150°) at 5, 10, 15, 20, 25, 30, 40, 50,  
134 70 and 100 meters above the bottom (mab). These instruments were programmed to measure  
135 turbidity, expressed in Formazin Turbidity Units (FTU), at 1-min intervals in auto-gain mode.  
136 The mooring line was also equipped with a downward-looking 300 kHz Teledyne RDI  
137 Acoustic Doppler Current Profiler (ADCP) placed above the turbidimeters. Unfortunately,  
138 during 2010 the ADCP did not record data due to a technical issue affecting the Firmware  
139 5x.37-5x.39 of RDI Workhorse sentinel platforms (Teledyne Field Service Bulletin FSB-194;  
140 08/11/2010) and the 20 mab turbidimeter ceased prematurely to record due to a problem with  
141 the batteries. The same site was reoccupied from 10 May to 12 October 2011. In this occasion,  
142 3 turbidimeters were placed at 5, 20 and 50 mab and the ADCP provided valid current data  
143 from 12 to 78 mab in 2 m-wide bins at 5-min intervals. The N-E current components were  
144 rotated to obtain along- and across-slope components taking into account the main orientation  
145 of the tributary valley ( $191^{\circ}$  from North). To complement these measurements with  
146 observations of the horizontal distribution of resuspended particles in the water column, a  
147 CTD transect (see Fig. 1 for CTD cast positions) crossing the northern canyon flank was  
148 conducted on 11 May 2011 after the end of the daily trawling activity. A Seabird SBE 911  
149 CTD probe equipped with a Seapoint turbidimeter was used.

150

151 FTU readings from the CTD and moored turbidimeters were converted to estimates of  
152 suspended sediment concentration (SSC) after the general calibration by Guillén et al. (2000):  
153  $SSC \text{ (mg l}^{-1}\text{)} = 1.74 \times (FTU - FTU_{\min})$ ,  
154 where  $FTU_{\min}$  is the minimum turbidity recorded by the sensor during a given deployment  
155 period.

156

157

158

159

### 160 **3. Results**

161

162 Figure 2 presents the complete time-series of SSC measured by selected turbidimeters from  
163 both years/deployments 2010 and 2011. An 18-day zoom from each of the two monitored  
164 years is shown in Figures 3 and 4 respectively, the latter also including current speed and  
165 direction.

166

#### 167 **3.1. Suspended sediment concentrations in the Montgrí tributary**

168

169 The time-series of SSC at the sampling site document the occurrence of frequent events of  
170 very high turbidity, reaching near-bottom SSCs of more than  $100 \text{ mg l}^{-1}$  (Fig. 2). These events  
171 were recorded only during working days of the local trawling fleet, while turbidity remained  
172 low during weekends and holidays (Figs. 3, 4). Several consecutive peaks of SSC were often  
173 observed in a same working day between 8 h and 16 h UTC. The suspended sediment  
174 increases occurred sharply, as SSC peaks 1-2 orders of magnitude above background values  
175 of  $\sim 1\text{-}3 \text{ mg l}^{-1}$ , and then faded out in the following few hours. Water turbidity during these

176 events increased first close to the bottom and was then subsequently observed propagating  
177 upwards in a few minutes, often reaching the topmost turbidimeter (100 mab in 2010; 50 mab  
178 in 2011). Maximum SSCs recorded by the bottommost turbidimeter (5 mab) during each  
179 deployment were  $180 \text{ mg l}^{-1}$  on 2 July 2010 (11:30 h UTC) and  $236 \text{ mg l}^{-1}$  on 24 May 2011  
180 (13:46 h UTC).

181 During the 2010 deployment, high turbidity events were particularly frequent and intense  
182 during the first month of measurements (July), and tended to weaken progressively along the  
183 following months. Nonetheless, SSC peaks in the range  $10\text{-}30 \text{ mg l}^{-1}$  were still measured in  
184 late summer. The 2011 recording period started earlier in the year (May) allowing to  
185 complement the previous temporal trend. In this case, suspended sediment peaks also tended  
186 to decrease in frequency and concentration towards autumn, and were maximal during late  
187 spring-early summer (Fig. 2).

188 A detailed view of the shape and daily evolution of consecutive resuspension plumes recorded  
189 during a working day is given in Figure 5, where turbidity data from 10 depths is integrated  
190 from 0 to 24 h of Friday 2 July 2010. From midnight to 8 h UTC, water turbidity remained  
191 below  $4 \text{ mg l}^{-1}$  from 5 to 20 mab and below  $2 \text{ mg l}^{-1}$  from 20 to 100 mab. Some minutes  
192 before 9 h UTC, a sharp increase of turbidity was observed to a minimum height of 70 mab  
193 (SSC in the range  $20\text{-}50 \text{ mg l}^{-1}$ ). At 11:30 near-bottom SSC peaked at  $180 \text{ mg l}^{-1}$  and  
194 subsequent relatively high turbidity bursts occurred until 15-16 h UTC (Fig. 5). During these  
195 high turbidity events, SSC increased first near the bottom and the signal propagated upwards  
196 afterwards. Towards the end of the working day, SSC progressively faded out near the bottom,  
197 and around 20:30 h UTC the suspended sediment plume was apparently detached from the  
198 seafloor, showing higher concentrations at mid-water depths between 50 and 100 mab, while  
199 turbidity near the seafloor was lower (Fig. 5).

200



201

### 202 **3.2. Near-bottom currents**

203

204 The speed and direction of water currents measured by the ADCP during a period  
205 representative of the 2011 mooring deployment are shown in Figure 4, while the across- and  
206 along-gully components of current speed are shown in detail together with SSC during two  
207 working days in Figure 6. Increases of current speed in the range 20-40 cm s<sup>-1</sup> were coherent  
208 with high SSC events and, like these, matched the time schedule of trawling activities. The  
209 ADCP measurements also showed higher velocities near the bottom, decreasing upwards (Fig.  
210 4). Such maximum velocities were oriented along the gully and down-slope, in agreement  
211 with the development of sediment gravity flows, while the across-gully component during  
212 these events was less clearly oriented and showed values <12 cm s<sup>-1</sup> (Fig. 6). On occasions,  
213 the simultaneous increases of down-gully current speed and SSC were restricted to <50 mab  
214 while, above, the water flow was reversed and directed up-slope, suggesting a compensation  
215 flow in the opposite direction of the gravity current (see second turbidity peak in Fig. 6).  
216 Outside events of high turbidity, current speed remained below 10 cm s<sup>-1</sup> (Fig. 4).

217

### 218 **3.3. Daily evolution of SSC**

219

220 Figure 7 integrates all the available SSC data at selected heights above the bottom from each  
221 deployment, ordered by the time of day. The time-averaged water turbidity at 5-50 mab  
222 increases abruptly around 8 h UTC in agreement with the passage of the trawling fleet  
223 upslope of the mooring site. Time-averaged maximum turbidity values at 100 mab show an  
224 apparent delay of several hours with respect to near-bottom values, although instantaneous  
225 SSC increases occurred often simultaneously during high turbidity events. The distribution of

226 high turbidity events is roughly bimodal in 2011, with one maximum centred on 9-10 h UTC  
227 and a second one around 14 h UTC. The first peak roughly corresponds to the time when the  
228 trawling fleet goes offshore and the second one when it heads back to port. This bimodal trend  
229 is less obvious in 2010 but still visible. After the end of the trawling period (15-16 h UTC),  
230 turbidity values drop steadily towards daily minimum values just before trawling activities are  
231 resumed the following day.

232

### 233 **3.4. CTD transect across the Sant Sebastià fishing ground**

234

235 Vertical profiles of hydrographic parameters and suspended sediment concentration from a  
236 CTD transect across the Sant Sebastià fishing ground are shown in Figure 8. This transect was  
237 carried out at the end of a working day (11 May 2011), eastwards from the mooring site and  
238 outside any identifiable canyon tributary valley (Fig. 1). A conspicuous bottom nepheloid  
239 layer (BNL) was observed at the profiles intersecting the range of fishing depths (station 3  
240 and 4). In particular, a 20 m thick BNL with SSC increasing towards the seafloor up to  
241 maximum  $\sim 5.0 \text{ mg l}^{-1}$  at 5 mab (according to the altimeter) was observed at station 3 (670 m  
242 depth). At station 4 (498 m depth) a 43 m thick BNL with maximum SSC  $3.8 \text{ mg l}^{-1}$  was also  
243 present. This BNL appears to detach from the canyon flank and generate the intermediate  
244 nepheloid layer (INL) observed at 500-600 m depth in station 3. No obvious INL detachments  
245 were observed deeper inside the main canyon valley (stations 1 and 2), although a slightly  
246 higher water turbidity was observed at 700-1100 m depth. An additional INL was apparent at  
247 the shallowest stations 4-6 between 150 and 220 m depth (i.e., at shelf-break depths) and  
248 constrained by the density gradient between Atlantic Waters and Levantine Intermediate  
249 Waters (Fig. 8).

250

251

252 **4. Discussion**

253

254 **4.1. Trawling-induced resuspension events**

255

256 The time-series of suspended sediment concentration in the Montgrí tributary valley revealed  
257 the occurrence of frequent events of very high turbidity, induced by trawling as evidenced by  
258 the tight coupling between the temporal distribution of these events and the working schedule  
259 of the fishing fleet operating in the neighbouring fishing ground (Figs. 3, 4, 7).

260

261 The downslope sediment transport events detected deeper than the fishing grounds are  
262 attributable to the generation of sediment gravity flows (i.e. flows by which water moves  
263 downslope due to the contribution of suspended sediment load to the density of the fluid,  
264 creating negative buoyancy; see Middleton and Hampton, 1976). Such type of flows were  
265 identified by measurements from single point current meters deployed in 2001 at the  
266 confluence of the Montgrí tributary valley with La Fonera canyon axis (Palanques et al., 2006)  
267 and confirmed by currents recorded by the ADCP deployed during this study (Puig et al.,  
268 2012; Figs. 4, 6). This rapid flushing of sediments through the tributary valley causes the  
269 sharpness of turbidity increases, the subsequent propagation of the signal from the bottom  
270 upwards and the relatively fast fading out of the turbid signal afterwards (Fig. 5). The high-  
271 turbidity events observed in the tributary had a frequency and intensity that surpassed our  
272 previous observations. Events with an almost daily recurrence and near-bottom sediment  
273 loads up to  $236 \text{ mg l}^{-1}$  at 5 mab in the Montgrí tributary valley at 980 m depth contrast with  
274 more sporadic and less turbid events (maximum  $30 \text{ mg l}^{-1}$  at 12 mab) measured in the canyon  
275 axis at 1200 m depth by Palanques et al. (2006).

276

277 The lack of any significant resuspension event outside working days and working hours in  
278 284 days of continuous recordings (Figs. 3, 4, 7) testifies to the weakness or rarity of natural  
279 processes capable of producing similar effects at this location and depth. Consequently, we  
280 can assert that the present-day near-bottom water turbidity in the Montgrí tributary valley is,  
281 both in timing and magnitude, basically anthropogenic. The consistence of observations  
282 between two consecutive years further indicates a durable situation of altered natural patterns,  
283 which could have been occurring since 1960s-1970s as inferred by changes in sediment  
284 accumulation rates within the canyon axis linked to the increase of total engine power of the  
285 trawling fleet working in the study area (Martín et al., 2008).

286

287 The thickness of the sediment plumes generated by the sediment gravity flows, often  
288 extending 100 m above the bottom, is also remarkable. In the Gulf of Lions shelf, Durrieu de  
289 Madron et al. (2005) reported trawling-induced bottom nepheloid layers (BNL) 3-6 m thick  
290 with average SSC of 50 mg l<sup>-1</sup> close to the bottom, rapidly declining upwards. Palanques et al.  
291 (2001) on the inner shelf off Barcelona measured SSC increasing up to 6 mg l<sup>-1</sup> and BNL  
292 thickness up to 15 m after the passage of otter trawlers. These observations conducted in  
293 continental shelf environments indicate lower concentrations and thinner turbid plumes  
294 compared with the much higher sediment loads reaching greater distances above the bottom  
295 observed in this study. This fact seems to confirm the previously held (but largely  
296 unsupported by direct observations) idea that trawling fisheries at slope depths might produce  
297 greater physical impacts than shallow-water correlatives. To account for these large  
298 differences, first it must be taken into account that deep-sea trawling in general requires  
299 heavier and bigger gears dragged by more powerful engines than shallow water counterparts,  
300 resulting in an enhanced capacity to impact the seafloor (e.g. Ragnarsson and Steingrímsson,

2003). Also, the sediment grain size of surface sediments tends to be finer on continental slopes than on shelves, hence, clouds of resuspended particles could have longer residence times in the water column in the former case. Surface sediments at the Sant Sebastià fishing ground near the Montgrí gully are basically composed of silty mud, with sand contents <3% (mean  $\phi = 7.4$ ) (unpublished results). Additionally, steeper bathymetries of continental slopes, and in particular on the rims of submarine canyons, compared to gently-sloping shelves, can promote sediment gravity flows, while the topographic constrain of the tributary valley may act as a funnel, focusing and channelling resuspended particles toward greater depths. Such factors contribute to promote sediment gravity flows and further enhance the propagation of resuspended sediments far from their source.

311

#### 312 **4.2. Seasonal evolution of water turbidity in the Montgrí tributary**

313

314 A remarkable aspect of the turbidity time series recorded in the Montgrí tributary valley is the  
315 decline in frequency and intensity of high-turbidity episodes from late spring/early summer  
316 through autumn (Fig. 2). This temporal trend is coherent with previous observations of  
317 downward particle fluxes in the canyon axis at 1200 m depth downslope from the Montgrí  
318 tributary valley), which were high from May to July 2001 and declined markedly from mid-  
319 August (Martín et al., 2006). It also makes sense in light of the general mobility patterns of  
320 the fishing fleet, which in turn follows the seasonal displacements of the targeted species.  
321 *Aristeus antennatus* tends to form aggregations at depths of 400-900 m during the  
322 reproductive period in spring and early summer, and moves to shallower depths by late  
323 summer (Sardà et al., 1994), being fished at 400-600 m from autumn through winter  
324 (Demestre and Martín, 1993) The spring-early summer deep aggregations are mainly

325 composed of highly priced mature females, hence maximum captures and working depths  
326 take place during that period (Demestre and Martín, 1993; Tobar and Sardà, 1987).

327

328 It is worth to note that the data set shown in Fig. 2 suggests a disruption of the general annual  
329 cycle of sediment transport in the Northwest Mediterranean continental margin, where  
330 particle fluxes tend to be higher in autumn-winter and lower in spring-summer due to the  
331 seasonal dynamics of the coastal and slope currents and the occurrence of storms and river  
332 discharges (Heussner et al., 1996). Changes in the annual trends of sediment resuspension as a  
333 consequence of trawling activities were also noted by Floderus and Pihl (1990) at shallow  
334 depths in the Kattegat.

335

#### 336 **4.3. Can bottom trawling contribute to feed nepheloid layers?**

337

338 Hydrographical profiles conducted after the passage of the trawling fleet over the Sant  
339 Sebastià fishing ground reveal the presence of slope BNLs and detachments of INLs from the  
340 canyon flank (Fig. 8). At the shallowest stations 4-6 a diluted INL is apparent at  
341 approximately 150-220 m depth, likely generated by natural processes causing detachments of  
342 suspended particles at the shelf-break that spread constrained by the density gradient between  
343 Atlantic Water (AW) and Levantine Intermediate Water (LIW). On the other hand, the well  
344 developed and concentrated ( $4\text{-}5\text{ mg l}^{-1}$ ) BNL and the deep INL recorded in the area where  
345 trawling takes place (stations 3 and 4) are likely related to trawling-induced resuspension. The  
346 across-canyon transect shown in Figure 8 was conducted at the end of a working day and  
347 hence reflects turbidity values corresponding to the aftermath of the passage of trawling gears.

348

349 Observations at the mooring site reveal that the residual part of the sediment that remains in  
350 suspension after the passage of the sediment gravity flows contribute to feed a BNL,  
351 maintaining relatively high turbidity values near the seafloor for several hours until the  
352 trawling activities resume the day after (Fig. 7). Additionally, the lighter and presumably finer  
353 fraction of the resuspended particles tends to be detached from the seafloor and uplifted into  
354 the water column at the end of a working day (Fig. 5), contributing to the development of an  
355 INL at mid water depths. In fact, the INL detachment observed at station 3 around 500-600 m  
356 depth seems to be generated by trawling activities in shallower areas (around station 4) from  
357 where resuspended particles could be detached and retained by the density gradient between  
358 the Levantine Intermediate Water (LIW) and the Western Mediterranean Deep Water  
359 (WMDW) (Fig. 8).

360

361 Internal waves being propagated along shelf-slope density fronts have been proposed as a  
362 mechanism to create resuspension and/or maintenance of particles in suspension generating  
363 nepheloid layers in continental slope regions, which tend to be detached from the seafloor into  
364 the ocean interior (Gardner, 1989; Puig and Palanques, 1998; Puig et al., 2004; McPhee-  
365 Shaw, 2006). Our data suggest that besides internal wave activity, resuspension induced by  
366 trawling gears can also play a significant role as initiator of sediment resuspension at slope  
367 depths generating localized bottom and intermediate nepheloid layers over and around fishing  
368 grounds. The fact that the intermediate nepheloid layer detachments on the La Fonera canyon  
369 flank were not observed in the deepest hydrographic stations (1 and 2 in Fig. 8) suggests that  
370 the resuspended particles are preferentially advected along-margin by ambient currents,  
371 following the isobaths, despite the fact that such currents show relatively weak velocities ( $<10$   
372  $\text{cm s}^{-1}$ ; Fig. 6).

373

374 These observations are also consistent with a previous study, where a set of CTD profiles  
375 collected in 2001 (Palanques et al., 2005) suggested enhanced near-bottom turbidity on the  
376 northern canyon flank during spring-summer. Zúñiga et al. (2009) also observed in the  
377 neighbouring Blanes Canyon (where the *Aristeus antennatus* fishery is also active at similar  
378 depths) a consistent intermediate nepheloid layer at 600-800 m depth detaching from the  
379 eastern canyon flank.

380

#### 381 **4.4. Ecological consequences and global implications**

382

383 Deep-sea ecosystems are in general adapted to a limited variability of physical conditions,  
384 resulting in a high vulnerability to artificial changes in their habitats, matter and energy inputs  
385 or hydrodynamic stress (Glover and Smith, 2003). Consequently, increases of water turbidity  
386 2 orders of magnitude above the background levels and the replacement of natural cycles in  
387 temporal scales from diurnal to annual by a man-made schedule, as observed in this study,  
388 must have favoured adaptation strategies and communities different to those inhabiting the  
389 study area before intensive trawling times. Our observations also confirm that the effects of  
390 bottom trawling can propagate downslope from the areas actually exploited by trawlers,  
391 affecting larger and deeper areas. An extension of trawling impacts beyond fishing grounds  
392 has been documented in the NE Atlantic by Priede et al. (2011), who observed that the total  
393 abundance of demersal fishes had decreased 1000 m downslope from the trawled depth range  
394 (500-1500 m depth). Priede et al. (2011) invoked the removal of eurybathic deep-sea fishes at  
395 the shallow end of their depth range to explain the observed decrease in fish abundance.  
396 Without contradicting that interpretation, our results also suggest that trawling-induced  
397 physical impacts themselves can also propagate downslope from fishing grounds as sediment  
398 gravity flows and eventually as nepheloid layers. This could in turn compromise the survival



399 rates of deep-sea animals through suffocation and clogging of respiratory surfaces or by  
400 preventing the normal settlement of larvae, among other effects that may derive from a  
401 substantial change in the amount of suspended solids in the water column (Jones, 1992). This  
402 may have as well implications for the management of the deep-sea and the definition of  
403 protected areas. Conservation measures such as the ban on bottom trawling beyond the 1000-  
404 m isobath, recommended by the General Fisheries Council for the Mediterranean in 2005  
405 (GFCM, 2005), might not be enough to guarantee the protection of vulnerable deep-sea  
406 ecosystems below that depth.

407

408 Deep-sea fisheries at slope depths and in the vicinity of steep environments such as submarine  
409 canyons, ridges and seamounts are not exclusive of the study area but fairly widespread and  
410 recently estimated as 4.4 million km<sup>2</sup> only on continental slopes (Puig et al., 2012) and 20  
411 million km<sup>2</sup> comprising all marine trawled areas (World Resources Institute, 2000). In the  
412 light of these facts, the global scale implications of bottom trawling activities for deep-sea  
413 ecosystems and biogeochemical cycles deserve further interest from the scientific community.

414

## 415 **5. Concluding remarks**

416

417 This study conducted in the La Fonera (=Palamós) Canyon at 980 m depth showed that  
418 commercial trawling on the northern canyon flank controls water turbidity in a neighbouring  
419 tributary to at least 100 m above the bottom. Trawling-induced resuspension causes turbidity  
420 increases near the bottom up to 2 orders of magnitude higher than background levels. No  
421 significant increases in turbidity were recorded outside working hours and working days,  
422 implying that natural processes capable of resuspending sediments are weak at the mooring  
423 site, and consequently, that man-made resuspension is the major driver of sediment dynamics.

424 This study also suggests that, aside from the generation of sediment gravity flows, bottom  
425 trawling can contribute to the development of slope nepheloid layers, and in this way, its  
426 effects can effectively propagate away from fishing grounds. Since deep-sea trawling is not  
427 exclusive of the study area but increasingly spread around the global ocean, the present study  
428 raises the alert whether natural patterns of sediment resuspension and water column turbidity  
429 in the deep sea are being replaced by a man-made schedule, with unknown consequences for  
430 global biogeochemical cycles and deep-sea ecosystems.

431

432

### 433 **Acknowledgements**

434

435 We are grateful to the crew and officers of B/O García del Cid (CSIC) and “Lluerna”  
436 (Generalitat de Catalunya) and to the participants in the HERMIONE-I & II surveys for their  
437 help at sea. This work is funded by the HERMIONE project (Grant agreement 226354) under  
438 the European Commission's 7th Framework Programme. J. Martín was funded through a JAE-  
439 DOC contract within the Program «Junta para la Ampliación de Estudios», granted by  
440 Consejo Superior de Investigaciones Científicas and co-financed by the European Social Fund.  
441 We thank the two anonymous reviewers who helped to improve the submitted manuscript  
442 through their constructive comments.

443

444

445

446

447

448

449 **References**

450

451 Alegret, J.L., Garrido, A., 2004. Historia de la Confraria de Pescadors de Palamós. Confraria  
452 de Pescadors de Palamós. Palamós, Spain.

453

454 Allen, S.E., Vindeirinho, C., Thomson, R.E., Foreman, M.G.G., Mackas, D.L., 2001. Physical  
455 and biological processes over a submarine canyon during an upwelling event. *Can. J. Fish.*  
456 *Aquat. Sci.* 58, 4411-4421.

457

458 Benn, A.R., Weaver, P.P., Billet, D.S.M., van den Hove, S., Murdock A.P., Doneghan, G. B.,  
459 Le Bas, T., Roopnarine, P., 2010. Human Activities on the Deep Seafloor in the North East  
460 Atlantic: An Assessment of Spatial Extent. *PLoS ONE* 5(9), e12730.  
461 doi:10.1371/journal.pone.0012730.

462

463 Bensch, A., Gianni, M., Greboval, D., Sanders, J., Hjort, A., 2009. Worldwide review of  
464 bottom fisheries in the high seas. *FAO Fisheries and Aquaculture Technical Paper Rome*.  
465 <ftp://ftp.fao.org/docrep/fao/011/i0540e/i0540e.zip>

466

467 Black, K.P., Parry, G.D., 1994. Sediment transport rates and sediment disturbance due to  
468 scallop dredging in Port Phillip Bay. *Mem. Queensl. Mus.* 36(2), 327-341.

469

470 Churchill, J.H., 1989. The effect of commercial trawling on sediment resuspension and  
471 transport over the Middle Atlantic Bight continental-shelf. *Cont. Shelf Res.* 9, 841-864.

472

- 473 Dellapenna, T.M., Allison, M.A., Gill, G.A., Lehman, R.D., Warnken, K.W., 2006. The  
474 impact of shrimp trawling and associated sediment resuspension in mud dominated, shallow  
475 estuaries. *Estuar. Coast. Shelf Sci.* 69(3-4), 519-530.  
476
- 477 Demestre, M., Martín, P., 1993. Optimum exploitation of a demersal resource in the western  
478 Mediterranean: the fishery of the deep-water shrimp *Aristeus antennatus* (Risso, 1816). *Sci.*  
479 *Mar.* 57(2-3), 175-182.  
480
- 481 Durrieu de Madron, X., Ferré, B., Le Corre, G., Grenz, C., Conan, P., Pujo-Pay, M., Bodiot,  
482 O., Buscail R., 2005. Trawling-induced resuspension and dispersal of muddy sediments and  
483 dissolved elements. *Cont. Shelf Res.* 25, 2387-2409.  
484
- 485 Fabri, M.-C., Pedel, L., Beuck, L., Galgani, F., Hebbeln, D., Freiwald, A., 2013. Vulnerable  
486 Marine Ecosystems in French Continental Mediterranean Submarine Canyons: Spatial  
487 Distribution and Anthropogenic Impacts. *Deep-Sea Res. II* (this issue).  
488
- 489 Ferré, B., Durrieu de Madron, X., Estournel, C., Ulses, C., Le Corré, G., 2008. Impact of  
490 natural (waves and currents) and anthropogenic (trawl) resuspension on the export of  
491 particulate matter to the open ocean: application to the Gulf of Lion (NW Mediterranean).  
492 *Cont. Shelf Res.* 28, 2071-2091.  
493
- 494 Floderus, S., Pihl, L., 1990. Resuspension in the Kattegat: Impact of variation in wind climate  
495 and fishery. *Estuar. Coast. Shelf Sci.* 31(4), 487-498.  
496

497 Gardner, W.D., 1989. Periodic resuspension in Baltimore Canyon by focusing of internal  
498 waves. *J. Geophys. Res.* 94, 18185-18194.

499

500 GFCM, 2005. REC.CM-GFCM/29/2005/1. Management of certain fisheries exploiting  
501 demersal and deepwater Species.  
502 [ftp://ftp.fao.org/FI/DOCUMENT/gfcm/web/GFCM\\_Recommendations2005.pdf](ftp://ftp.fao.org/FI/DOCUMENT/gfcm/web/GFCM_Recommendations2005.pdf)

503

504 Glover, A.G., Smith. C.R., 2003. The deep-sea floor ecosystem: current status and prospects  
505 of anthropogenic change by the year 2025. *Environ. Conserv.* 30, 219-241.

506

507 Guillén, J., Palanques, A., Puig, P., Durrieu de Madron, X., Nyffeler, F., 2000. Field  
508 calibration of optical sensors for measuring suspended sediment concentration in the western  
509 Mediterranean. *Sci. Mar.* 64, 427-435.

510

511 Heussner, S., Calafat, A., Palanques, A., 1996. Quantitative and qualitative features of particle  
512 fluxes in the North-Balearic Basin, in: Canals, M., Casamor, J.L., Cacho, I., Calafat, A.,  
513 Monaco, A. (Eds.), EUROMARGE-NB Final Report, MAST II Programme, EU, vol. II, pp.  
514 41-66.

515

516 Jones, J.B., 1992. Environmental impact of trawling on the seabed: A review. *N. Z. J. Mar.*  
517 *Freshw. Res.* 26, 59-67.

518

519 Kaiser, M.J., Collie, J.S., Hall, S.J., Jennings, S., Poiner, I.R., 2002. Modification of marine  
520 habitats by trawling activities: prognosis and solutions. *Fish Fish.* 3(2), 114-136.

521

- 522 Lastras, G., Canals, M., Amblas, D., Lavoie, C., Church, I., De Mol, B., Duran, R., Calafat,  
523 AM., Hughes-Clarke, JE., Smith, CJ., Heussner, S., 2011. Understanding sediment dynamics  
524 of two large submarine valleys from seafloor data: Blanes and La Fonera canyons,  
525 northwestern Mediterranean Sea. *Mar. Geol.* 280(1-4), 20-39.
- 526
- 527 Main, J., Sangster, G.I., 1981. A study of sand clouds produced by trawl boards and their  
528 possible effect on fish capture. Scottish Fisheries Research Report No. 20. Dept of  
529 Agriculture and Fisheries for Scotland. 19 pp.
- 530
- 531 Martín, J., Palanques, A., Puig, P., 2006. Composition and variability of downward particulate  
532 matter fluxes in the Palamós submarine canyon (NW Mediterranean). *J. Mar. Syst.* 60, 75-97.
- 533
- 534 Martín, J., Palanques, A., Puig, P., 2007. Horizontal transfer of suspended particulate  
535 matter in the Palamós submarine canyon. *J. Mar. Res.* 65, 193-218.
- 536
- 537 Martín, J., Puig, P., Palanques, A., Masqué, P., García-Orellana, J., 2008. Effect of  
538 commercial trawling on the deep sedimentation in a Mediterranean submarine canyon. *Mar.*  
539 *Geol.* 252, 150-155.
- 540
- 541 McPhee-Shaw, E., 2006. Boundary-interior exchange: Reviewing the idea that internal-wave  
542 mixing enhances lateral dispersal near continental margins. *Deep-Sea Res. II* 53, 42-59.
- 543
- 544 Middleton, G.V., Hampton, M.A., 1976. Subaqueous sediment transport and depositional by  
545 sediment gravity flows, in: *Sediment Transport and Environmental Management*, Stanley,  
546 D.J., Swift, D.J.P. (Eds.), John Wiley, pp. 197-218.

547

548 Morato, T., Watson, R., Pitcher, T. J., Pauly, D., 2006. Fishing down the deep. *Fish. Fish.* 7,  
549 24-34.

550

551 Palanques, A., Guillén, J., Puig, P., 2001. Impact of bottom trawling on water turbidity and  
552 muddy sediment of an unfished continental shelf. *Limnol. Oceanogr.* 46, 1100-1110.

553

554 Palanques, A., García-Ladona, E., Gomis, D., Martín, J., Marcos, M., Pascual, A., Emelianov,  
555 M., Puig, P., Guillén, J., Gili, J.M., Tintoré, J., Jordi, A., Basterretxea, G., Font, J., Segura, M.,  
556 Blasco, D., Montserrat, S., Ruiz, S., Pagès, F., 2005. A multidisciplinary program to study the  
557 dynamics and the ecology of a Northwestern Mediterranean submarine canyon: The Palamós  
558 Canyon. *Prog. Oceanogr.* 66 (2-4), 89-119.

559

560 Palanques, A., Martín, J., Puig, P., Guillén, J., Company, J.B., Sardà, F., 2006. Evidence of  
561 sediment gravity flows induced by trawling in the Palamós (Fonera) submarine canyon  
562 (northwestern Mediterranean). *Deep-Sea Res. I* 53, 201-214.

563

564 Pilskaln, C.H., Churchill, J.H., Mayer, L.M., 1998. Resuspension of sediment by bottom  
565 trawling in the Gulf of Maine and potential geochemical consequences. *Conserv. Biol.* 12,  
566 1223-1229.

567

568 Priede, I.G., Godbold, J.A., Niedzielski, T., Collins, M.A., Bailey, D.M., Gordon, J.D.M.,  
569 Zuur, A.F., 2011. A review of the spatial extent of fishery effects and species vulnerability of  
570 the deep-sea demersal fish assemblage of the Porcupine Seabight, Northeast Atlantic Ocean  
571 (ICES Subarea VII). *ICES J. Mar. Sci.* 68(2), 281-289.

572

573 Puig, P., Palanques A., 1998. Nepheloid structure and hydrographic control on the Barcelona  
574 continental margin, northwestern Mediterranean. *Mar. Geol.* 149, 39-54.

575

576 Puig, P., Palanques, A., Guillén, J., El Khatab, M., 2004. Role of internal waves in the  
577 generation of nepheloid layers on the northwestern Alboran slope: Implications for  
578 continental margin shaping. *J. Geophys. Res.* 109, C09011.

579

580 Puig, P., Canals, M., Company, J.B., Martín, J., Amblas, D., Lastras, G., Palanques A.,  
581 Calafat, A., 2012. Ploughing the deep sea floor. *Nature* 489, 286-289.

582

583 Ragnarsson, S.A., Steingrímsson, S.A., 2003. Spatial distribution of otter trawl effort in  
584 Icelandic waters: comparison of measures of effort and implications for benthic community  
585 effects of trawling activities. *ICES J. Mar. Sci.* 60, 1200-1215.

586

587 Sardà, F., Cartes, J.E., Norbis, W., 1994. Spatio-temporal structure of the deep-water shrimp  
588 *Aristeus antennatus* (Decapoda: Aristeidae) population in the western Mediterranean. *Fishery*  
589 *Bulletin* 92 (3), 599-607.

590

591 Theil, H., Schriever, G., 1990. Deep-sea mining, environmental impact and the DISCOL  
592 project. *Ambio* 19, 245-250.

593

594 Tobar, R., Sardà, F., 1987. Análisis de la evolución de las capturas de gamba rosada, *Aristeus*  
595 *antennatus* (Risso, 1816), en los últimos decenios en Cataluña. *Inf. Técn. Inv. Pesq.* 142, 3-20.

596



597 Tragou, E., Zervakis, V., Papageorgiou, E., Stavrakakis, S., Lykousis, V., 2005. Monitoring  
598 the physical forcing of resuspension events in the Thermaikos Gulf-NW Aegean during 2001–  
599 2002. *Cont. Shelf Res.* 25, 2315–2331.

600

601 WWF/IUCN, 2004. The Mediterranean deep-sea ecosystems: an overview of their diversity,  
602 structure, functioning and anthropogenic impacts, with a proposal for conservation. IUCN,  
603 Málaga and WWF, Rome.

604

605 World Resources Institute, 2000. A guide to world resources 2000-2001: People and  
606 Ecosystems: the Fraying web of life, World Resources Institute, Washington, USA.

607

608 Würtz, M., 2012. Mediterranean Submarine Canyons: Ecology and Governance. International  
609 Union for the Conservation of Nature. Gland, Switzerland and Málaga, Spain.

610

611 Zúñiga, D., Flexas, M.M., Sanchez-Vidal, A., Coenjaerts, J., Calafat, A., Jordà, G., García-  
612 Orellana, J., Puigdefàbregas, J., Canals, M., Espino, M., Sardà, F., Company, J.B., 2009.  
613 Particle fluxes dynamics in Blanes submarine canyon (Northwestern Mediterranean). *Prog.*  
614 *Oceanogr.* 82, 239-251.

615

616

617

618

619

620

621

622 **Figure Captions**

623

624 **Figure 1.** Bathymetric chart of the La Fonera (=Palamós) submarine canyon in the  
625 Northwestern Mediterranean, showing the position of the mooring line (red diamond) in the  
626 Montgrí tributary valley deployed in 2010 and 2011. The main fishing ground (Sant Sebastià)  
627 on the northern canyon flank is marked as a shadowed area. Crosses indicate the positions of  
628 consecutive CTD casts carried out during 11 May 2011.

629

630 **Figure 2.** Time series of suspended sediment concentration (SSC) in the Montgrí tributary  
631 valley over a total water depth of 980 m depth during two consecutive sampling periods. a:  
632 SSC at 5, 25, 50 and 100 meters above the bottom (mab) from July to early November 2010;  
633 b: SSC at 5, 20 and 50 mab from May to mid October 2011.

634

635 **Figure 3.** Detail of the time series of suspended sediment concentration in the Montgrí  
636 tributary valley during 2010. “mab” stands for meters above the sea bottom. Days of the week  
637 are indicated in the timeline, working days are shadowed in blue.

638

639 **Figure 4.** Detail of the time series of suspended sediment concentration and current speed  
640 (ADCP) records in the Montgrí tributary valley during 2011. Days of the week are indicated  
641 in the timeline, working days are shadowed in blue. The rest period from 23 to 26 June 2011  
642 corresponds to the annual Palamos’ Town Festival. Minor ticks in the time axis mark 4-hour  
643 intervals.

644

645 **Figure 5.** Contour plot of suspended sediment concentration (single-point measurements at 5,  
646 10, 15, 20, 25, 30, 40, 50, 70, and 100 mab) in the Montgrí gully at 980 m water depth during

647 2 July 2010. Note the detachment of the turbid plume up into the water column after the  
648 passage of the sediment gravity flow.

649

650 **Figure 6.** Time series of current speed components (rotated along and across the direction of  
651 the main Montgrí tributary) and suspended sediment concentration at the Montgrí gully  
652 during 20-21 June 2011. Positive current speeds are directed down-slope and to the right  
653 when looking in a down-slope direction.

654

655 **Figure 7.** Integration of all SSC data (a: 1 July to 7 November 2010; b: 10 May to 12 October  
656 2011) at selected heights over the sea bottom, ordered by time of day. Instantaneous data  
657 (sampling rate = 1 min) are displayed as dots and 1-min averages in solid line. The range of  
658 working hours during fishing days of trawlers at the Sant Sebastià fishing ground is shown as  
659 a shaded area on the timeline.

660

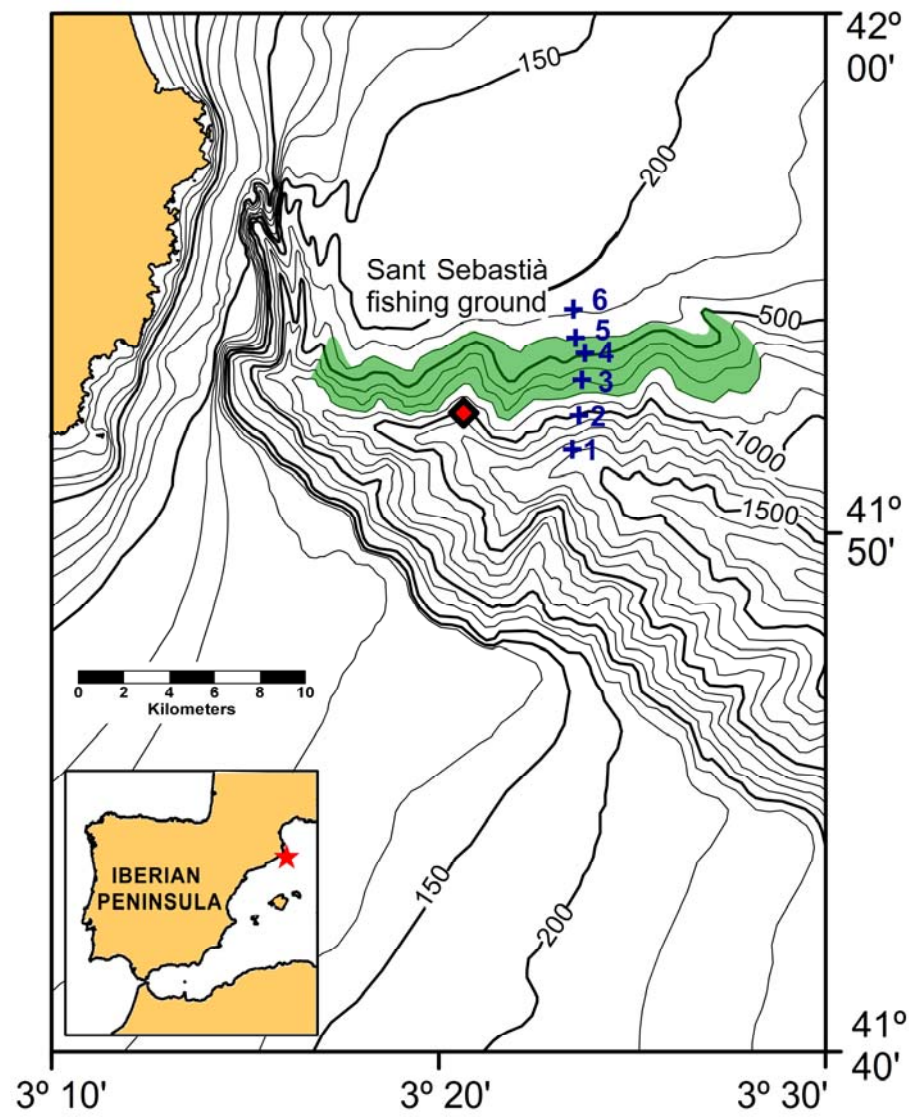
661 **Figure 8.** CTD vertical profiles of water potential temperature, salinity, potential density  
662 anomaly ( $\sigma\text{-theta}$ ), and suspended sediment concentration (SSC) from 100 m depth to 5  
663 meters above the seafloor, along a transect carried out on 11 March 2011 across the north  
664 flank of the La Fonera Canyon. The time (UTC) of cast start is given on top of the profiles.  
665 Shaded areas correspond to SSC values above the baseline at the depths of trawling activities  
666 (400-800 m) in the Sant Sebastià fishing ground. Note that only stations 3 and 4 are within the  
667 fishing ground (see Fig. 1 for positions of CTD stations). AW, LIW and WDMW stand for  
668 Atlantic Water, Levantine Intermediate Water and Western Mediterranean Deep Water  
669 respectively. INL= Intermediate nepheloid layer; BNL = Bottom nepheloid layer.

670

671

672 **Figure 1**

673



674

675

676

677

678

679

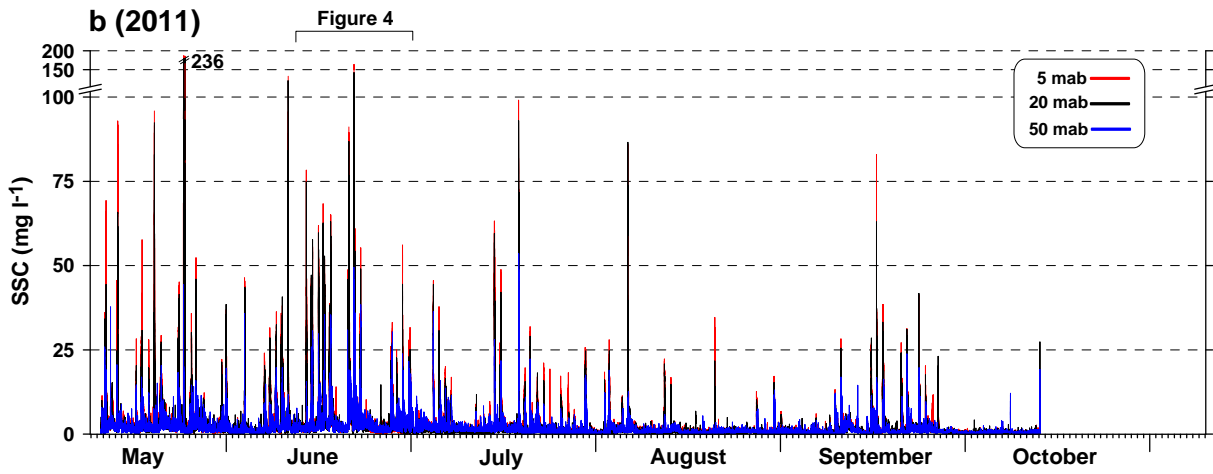
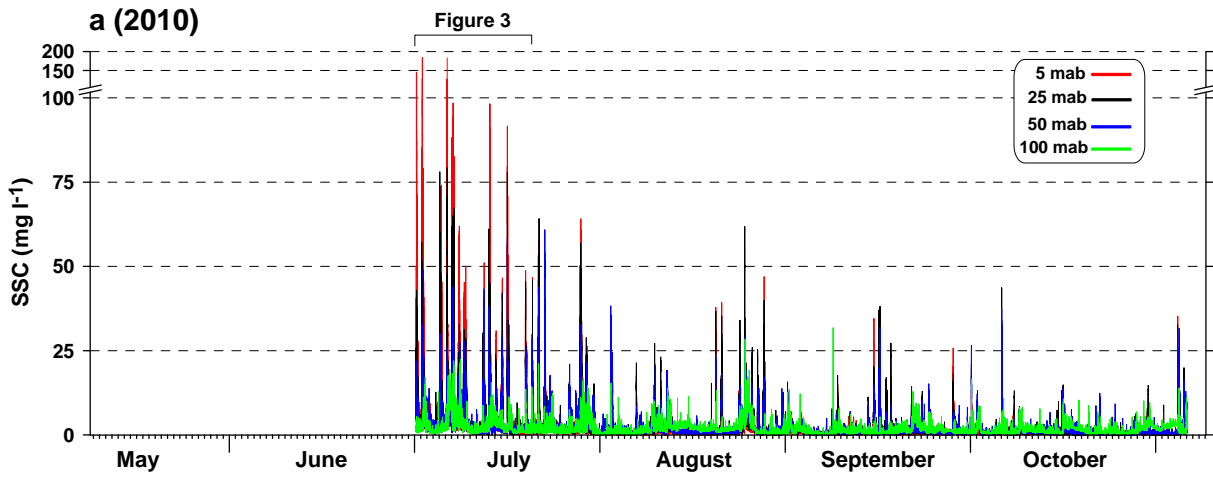
680

681

682

683 **Figure 2**

684



685

686

687

688

689

690

691

692

693

694

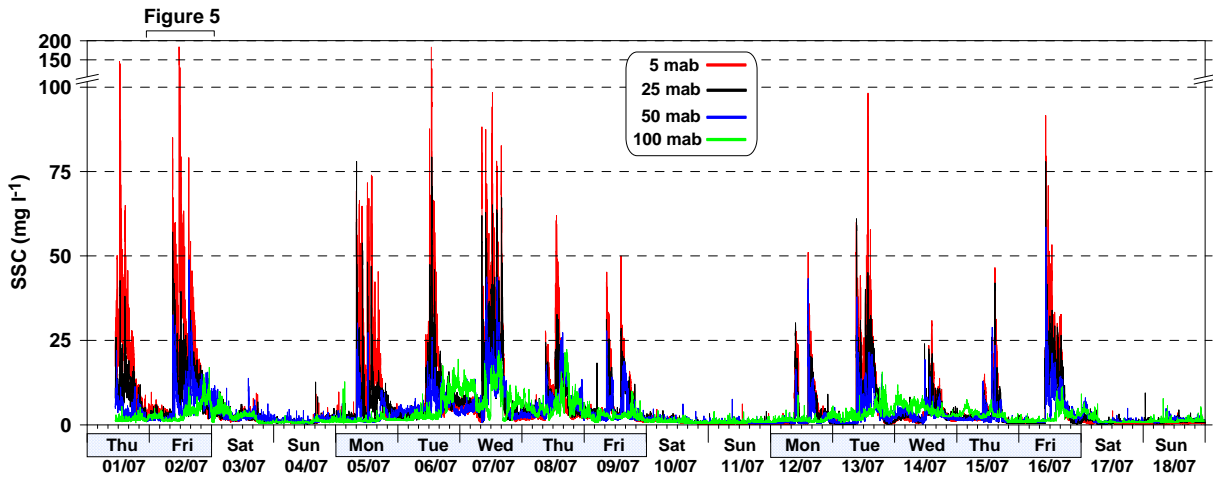
695

696

697

698 **Figure 3**

699



700

701

702

703

704

705

706

707

708

709

710

711

712

713

714

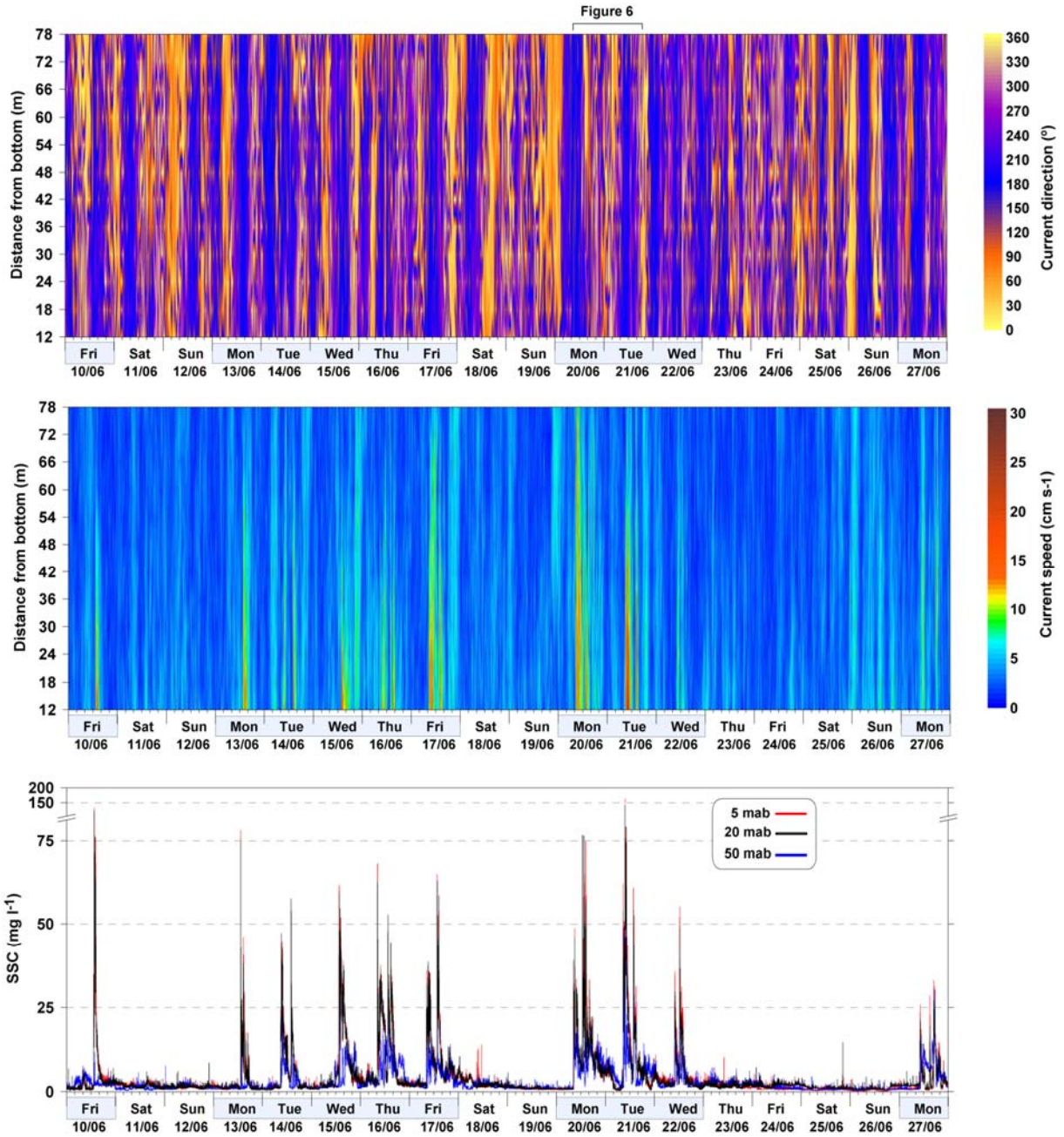
715

716

717

718 **Figure 4**

719



720

721

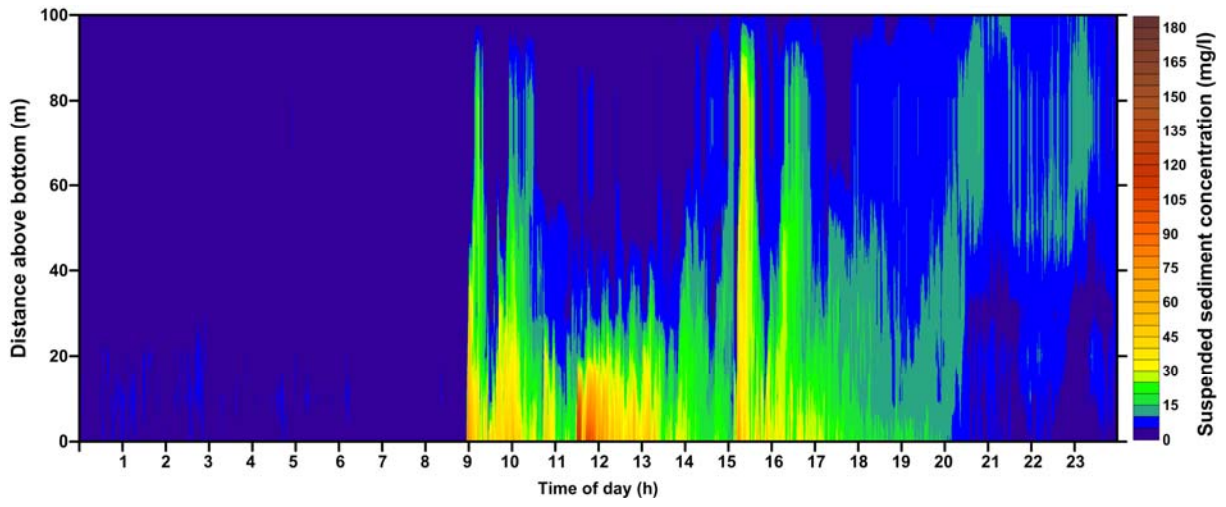
722

723

724

725

726 **Figure 5**



727

728

729

730

731

732

733

734

735

736

737

738

739

740

741

742

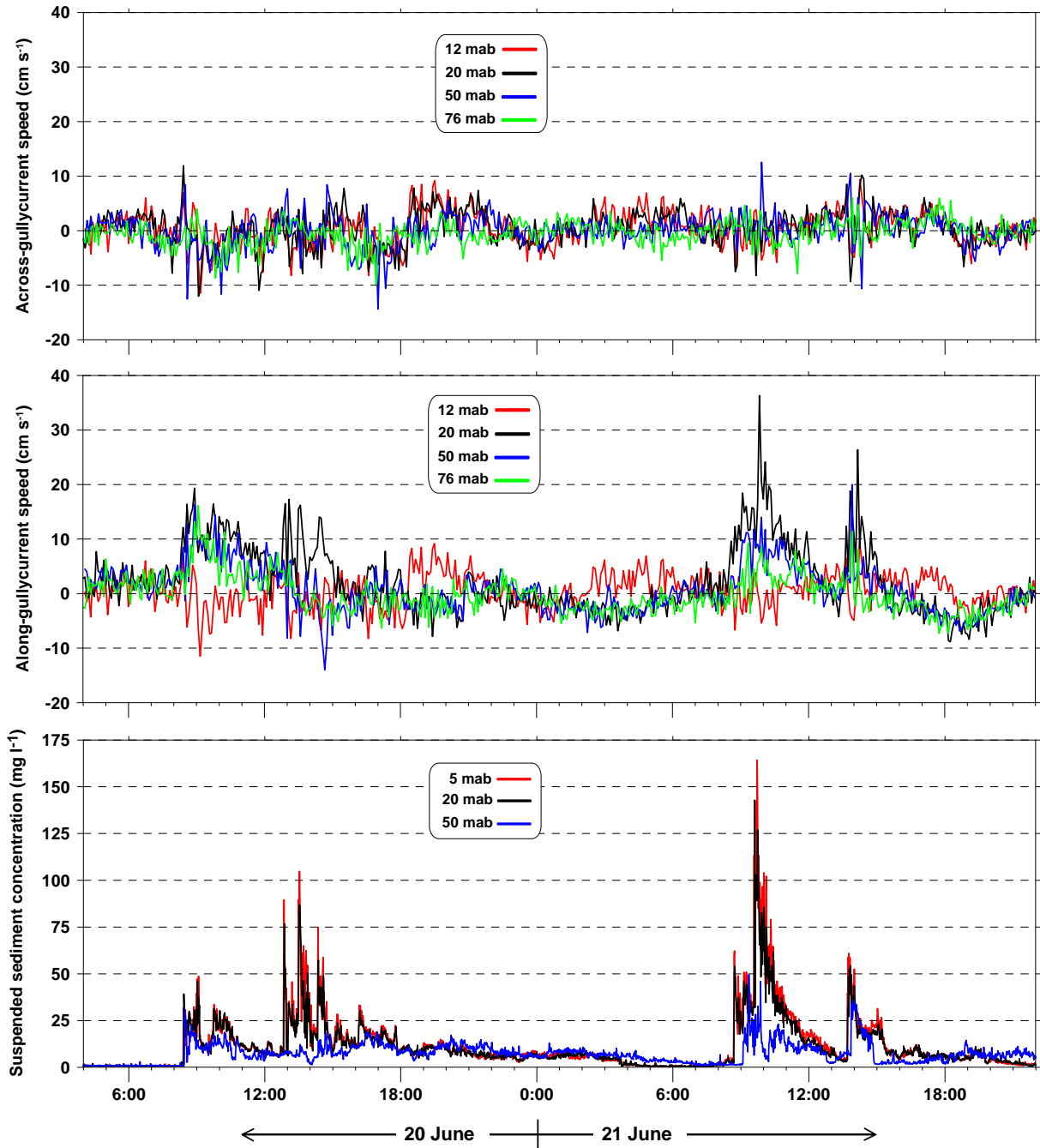
743



744

745 **Figure 6**

746



747

748

749

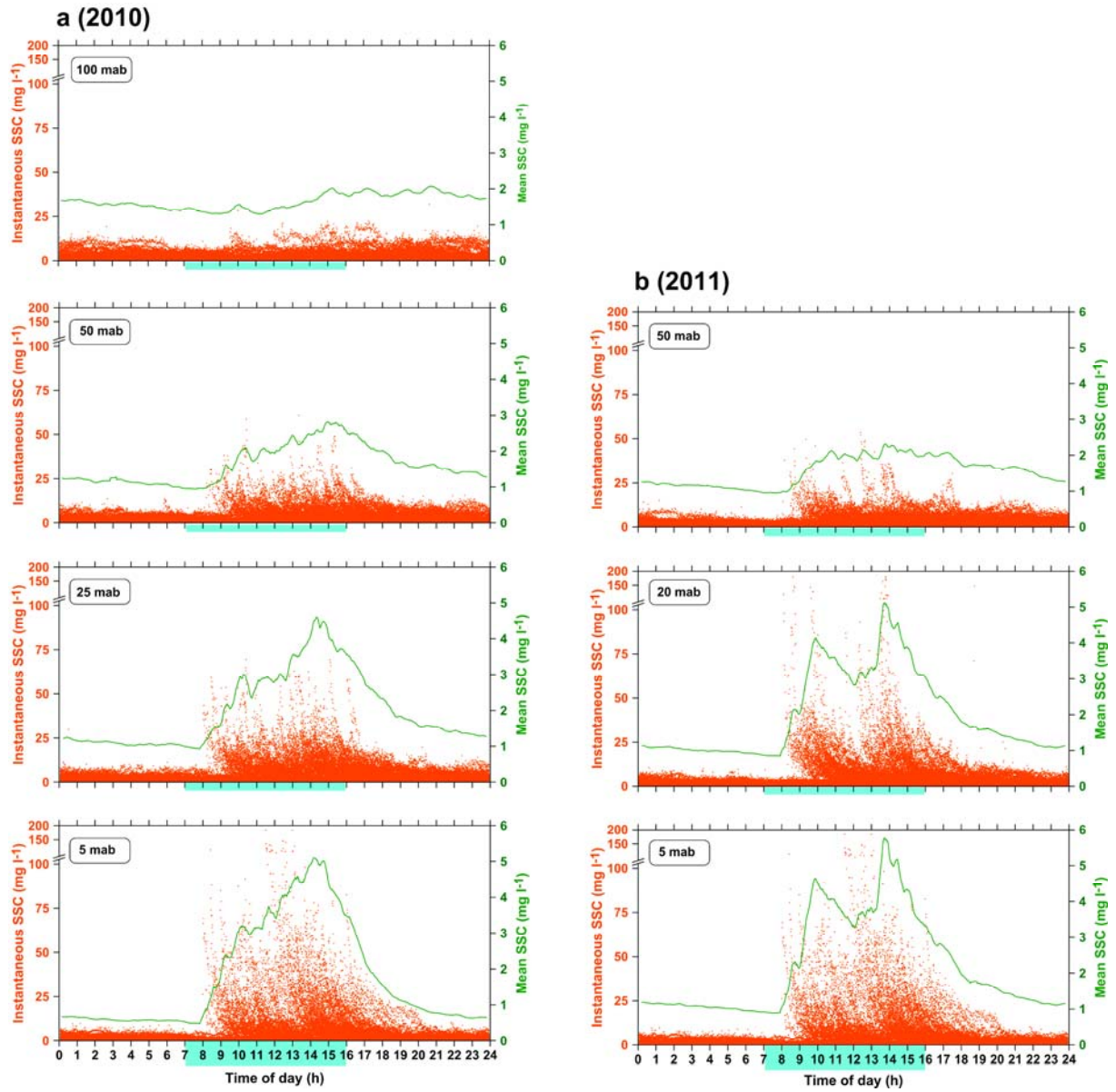
750

751

752

753 **Figure 7**

754



755

756

757

758

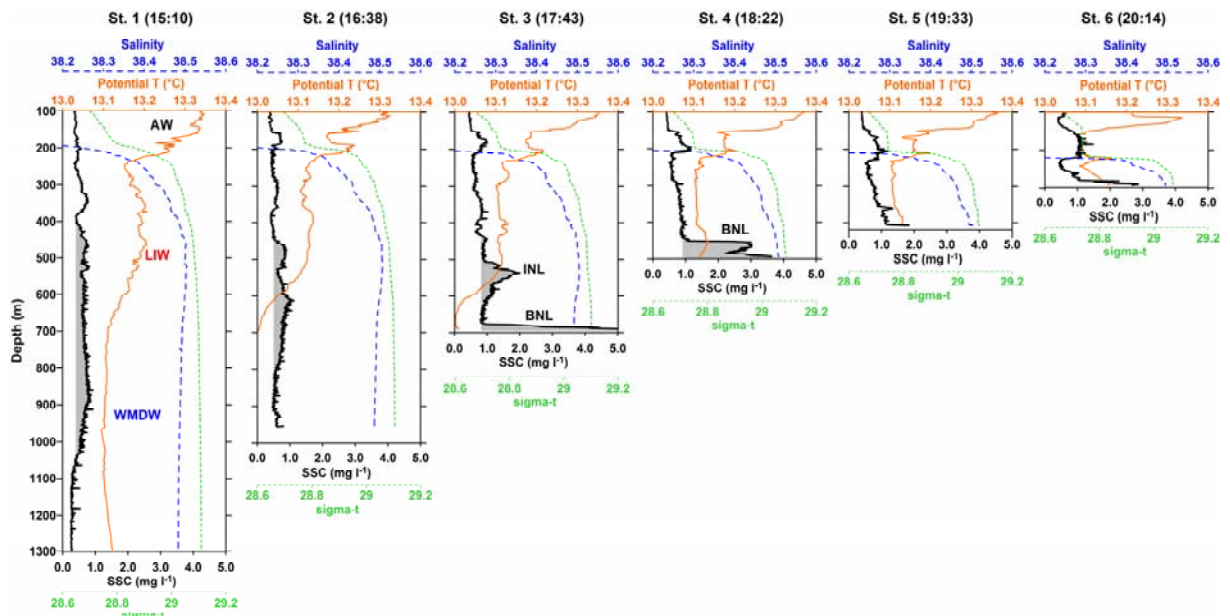
759

760

761

762

763 **Figure 8**



764

765

766

767

768

769

770

771

772